Identification of Ligand Binding Regions of the *Saccharomyces cerevisiae* α-Factor Pheromone Receptor by Photoaffinity Cross-Linking†

Cagdas D. Son,‡ Hasmik Sargsyan,§ Fred Naider,§,|| and Jeffrey M. Becker*,⊥

Department of Biochemistry, Cellular, and Molecular Biology, University of Tennessee, Knoxville, Tennessee 37996-0845, Department of Chemistry, College of Staten Island and Institute for Macromolecular Assemblies, City University of New York, Staten Island, New York 10314, Ph.D. Program in Biochemistry and Chemistry, The Graduate School and University Center of The City University of New York, 365 5th Avenue, New York, New York 10016, and Department of Microbiology and University of Tennessee-Oak Ridge National Laboratory School of Genome Science and Technology, University of Tennessee, Knoxville, Tennessee 37996-0845

Received February 11, 2004; Revised Manuscript Received August 10, 2004

ABSTRACT: Analogues of α-factor, *Saccharomyces cerevisiae* tridecapeptide mating pheromone (H-Trp-His-Trp-Leu-Gln-Leu-Lys-Pro-Gly-Gln-Pro-Met-Tyr-OH), containing *p*-benzoylphenylalanine (Bpa), a photoactivatable group, and biotin as a tag, were synthesized using solid-phase methodologies on a *p*-benzyloxybenzyl alcohol polystyrene resin. Bpa was inserted at positions 1, 3, 5, 8, and 13 of α-factor to generate a set of cross-linkable analogues spanning the pheromone. The biological activity (growth arrest assay) and binding affinities of all analogues for the α-factor receptor (Ste2p) were determined. Two of the analogues that were tested, Bpa[1] and Bpa[5], showed 3−4-fold lower affinity than the α-factor, whereas Bpa[3] and Bpa[13] had 7−12-fold lower affinities. Bpa[8] competed poorly with [^{3}H]-α-factor for Ste2p. All of the analogues tested except Bpa[8] had detectable halos in the growth arrest assay, indicating that these analogues are α-factor agonists. Cross-linking studies demonstrated that [Bpa[1]]-α-factor, [Bpa[3]]-α-factor, [Bpa[5]]-α-factor, and [Bpa[13]]-α-factor were cross-linked to Ste2p; the biotin tag on the pheromone was detected by a NeutrAvidin−HRP conjugate on Western blots. Digestion of Bpa[1], Bpa[3], and Bpa[13] cross-linked receptors with chemical and enzymatic reagents suggested that the N-terminus of the pheromone interacts with a binding domain consisting of residues from the extracellular ends of TM5−TM7 and portions of EL2 and EL3 close to these TMs and that there is a direct interaction between the position 13 side chain and a region of Ste2p (F55−R58) at the extracellular end of TM1. The results further define the sites of interaction between Ste2p and the α-factor, allowing refinement of a model for the pheromone bound to its receptor.

The yeast *Saccharomyces cerevisiae* is a sexual organism that manifests a conjugative response when opposite mating type cells, *MAT***a** and *MAT*α, are mixed together (for reviews, see refs *1*−*5*). The mating reaction is initiated by stimulation of cell surface receptors on each cell type by a polypeptide pheromone secreted from cells of the opposite mating type. Ste2p is a G protein-coupled receptor (GPCR)[1] expressed on the surface of haploid cells of the *MAT***a** mating type, which is involved in this initiation event. Binding of the α-factor tridecapeptide mating pheromone (Trp-His-Trp-Leu-Gln-Leu-Lys-Pro-Gly-Gln-Pro-Met-Tyr), secreted by the *MAT*α mating type, to Ste2p activates the pheromone signaling pathway by promoting dissociation of a coupled heterotrimeric G protein into its constituent α subunit and $\beta\gamma$ subunit complex on the cytoplasmic side of the plasma membrane. The activation of the receptor leads to a series of events, including G_1 growth arrest, cellular elongation, gene induction, agglutinin biosynthesis, and ultimately cell fusion with the opposite *MAT*α mating type cells.

GPCRs constitute a major family of human proteins (*6*). To date, more than 1000 GPCRs have been identified, and these proteins recognize diverse signaling molecules, including neurotransmitters, sensory molecules, and chemotactic agents (*7*). The ubiquitous nature of GPCRs together with their highly specific ligand recognition makes them an important target for therapeutic agents (*8*, *9*). Among the most important GPCR ligands are peptides, including hormones, growth factors, and pheromones. Understanding

† This work was supported by Grants GM22086 and GM22087 from the National Institutes of Health. F.N. holds the Leonard and Esther Kurtz Term Professorship at the College of Staten Island.

* To whom correspondence should be addressed. E-mail: jbecker@utk.edu. Phone: (865) 974-3006. Fax: (865) 974-4007.

‡ Department of Biochemistry, Cellular, and Molecular Biology, University of Tennessee.

§ City University of New York.

|| The Graduate School and University Center of The City University of New York.

⊥ University of Tennessee.

[1] Abbreviations: BNPS-skatole, 2-(2′-nitrophenylsulfenyl)-3-methyl-3′-bromoindolene; Bpa, 4-benzoyl-L-phenylalanine; BSA, bovine serum albumin; CNBr, cyanogen bromide; DIEA, *N*,*N*-diisopropylethylamine; ESI-MS, electron spray mass spectrometry; Fmoc, 9-fluorenylmethoxycarbonyl; GPCR, G protein-coupled receptor; HBTU, 2-(1*H*-benzotriazol-1-yl)-1,1,3,3-tetramethyluronium hexafluorophosphate; HOBt, *N*-hydroxybenzotriazole; NA−HRP, NeutrAvidin−horseradish peroxidase conjugate; Nle, norleucine; OBu^t, *tert*-butyl; tBoc, *tert*-butoxycarbonyl; TAME, *N*-α-*p*-tosyl-L-arginine methyl ester; TFA, trifluoroacetic acid; Wang resin, (4-hydroxymethyl)phenoxymethyl on 1% cross-linked polystyrene resin (bead).

10.1021/bi0496889 CCC: $27.50 © 2004 American Chemical Society
Published on Web 09/25/2004

the molecular mechanism of peptide recognition by their cognate GPCRs may lead to design of novel peptide analogues for treatment of disorders involving defective ligands and/or mutant receptors.

While there has been considerable literature on the GPCR ligand binding sites for small molecules such as biogenic amines (*10*), relatively less information concerning the binding sites of peptide-responsive GPCRs exists. Photoreactive cross-linking studies, using 4-benzoyl-L-phenylalanine (Bpa)-containing peptide ligands, are a powerful complement to site-directed mutagenesis studies for mapping peptide−receptor interaction(s). Studies reported on parathyroid hormone (PTH), opioid receptor (ORL1) (*11*−*17*), substance P (*18*−*20*), cholecystokinin (*21*), and vasopressin (*22*) showed that Bpa-containing peptides can be successfully used for identification of receptor fragments that are interacting with photoactivatable peptide analogues. Recent work on human PTH receptor (*23*, *24*), the secretin receptor (*25*), the ORL1 receptor (*26*), and the human angiotensin type I receptor (*27*) showed that specific contact residues can be mapped after photoaffinity labeling by sequencing of the cross-linked fragment and site-directed mutagenesis in the region of cross-linking. A new method called the methionine proximity assay took advantage of modified analogues of Bpa, e.g., *p*,*p*′-nitrobenzoylphenylalanine (NO_2Bpa), that exhibit selectivity for methionine residues (*28*). This unique property allowed the identification of a contact site by methionine scanning of the putative contact residues of three GPCRs, followed by analysis of the cross-linked receptor. All of these studies using Bpa analogues revealed that generation of covalently linked ligand−receptor conjugates has become a valuable tool for the identification of the cross-linked domains, allowing mapping of the interface between a peptide ligand and its GPCR (*29*).

Previously, we reported this general approach to identifying directly the interaction between position 1 of the α-factor and a region between residues 251 and 294 of the receptor Ste2p (*30*). However, that study was limited to the use of only one Bpa-bound α-factor analogue. Here we report the evaluation of a series of photoactivatable analogues containing Bpa at various positions throughout the α-factor pheromone. An important aspect of this study is the use of biotin as a tag allowing detection of cross-linking using avidin-based horseradish peroxidase (HRP) conjugates and eliminating problems previously encountered with radioactive iodine (*30*). Four analogues were selectively cross-linked into the α-factor binding site of Ste2p. Chemical and enzymatic fragmentation of the cross-linked receptor allowed us to identify contacts between the position 3 and 13 side chains of the pheromone and Ste2p residues in the EL2−TM5 and/or TM6−EL3−TM7 region and first transmembrane domain, respectively.

EXPERIMENTAL PROCEDURES

Organisms. S. cerevisiae DK102 [MAT**a** *ste2*::*HIS3 bar1 leu2 ura3 lys2 ade2 his3 trp1*] transformed with pNED1-[*STE2*] (*31*) was used in binding studies and in the growth arrest assays of various α-factor analogues. Strain BJ2168 was used as a parental strain to construct BJS21 by deleting *STE2* using the kanamycin deletion cassette according to a standard protocol (*32*). The BJS21 [MAT**a** *ste2*::*Kan*^{R}, *prc1-407, prb 1-1122, pep4-3, Leu2, trp1, ura 3-52*] strain transformed with pNED1[*STE2*] was used in cross-linking studies. All strains exhibited a similar binding of the α-factor. However, the BJS21 pNED strain lacked several peptidases, so it was used to increase the yield of Ste2p in experiments involving cross-linking.

Chemical Reagents. All reagents and solvents used for the solid-phase peptide synthesis of the photoactivatable peptides were analytical grade and were purchased from Advanced ChemTech (Louisville, KY), VWR Scientific (Piscataway, NJ), or Aldrich Chemical Co. (Milwaukee, WI). High-performance liquid chromatography (HPLC) grade dichloromethane (CH_2Cl_2), acetonitrile (ACN), methanol (MeOH), and water were purchased from VWR Scientific and Fisher Scientific (Springfield, NJ).

Synthesis of N-α-Fmoc-Protected α-Factor Analogues. N-α-Fmoc-protected α-factor analogues needed for the preparation of their biotinylated derivatives were synthesized by solid-phase peptide synthesis on an Applied Biosystems 433A peptide synthesizer (Applied Biosystems, Foster City, CA) starting with N-α-Fmoc-Tyr(OBu^t)- or N-α-Fmoc-Bpa-Wang resin (0.7 mmol/g substitution, Advanced ChemTech). In all of the peptides, L-norleucine (Nle), which is isosteric with L-methionine, was incorporated at position 12 to replace the naturally occurring L-methionine to prevent oxidation of the sulfur atom of this amino acid during peptide synthesis and purification. Replacement of Met with Nle was shown previously to result in an analogue with activity and receptor affinity equal to those of the native pheromone (*33*). Since all analogues have Nle in place of Met^{12}, this residue is eliminated from the abbreviated names for simplicity. The 0.1 mmol FastMoc chemistry of Applied Biosystems was used for the elongation of the peptide chain with an HBTU-, HOBt-, and DIEA-catalyzed, single coupling step using 10 equiv of protected amino acids for 30 min. Upon completion of chain assembly, the N-α-Fmoc group was not removed from the peptide chain.

Cleavage of the Peptide. The N-α-Fmoc-protected peptidyl resin was washed thoroughly with 1-methyl-2-pyrrolidinone and dichloromethane and dried in a vacuum for 2 h. The peptide was cleaved from the resin support with simultaneous side chain deprotection using a cleavage cocktail containing trifluoroacetic acid (10 mL), crystalline phenol (0.75 g), thioanisole (0.5 mL), and water (0.5 mL) at room temperature for 1.5 h with the omission of 1,2-ethanedithiol from the cleavage reaction, because it was known to transform Bpa-containing peptides to cyclic dithioketal derivatives (*34*). The filtrates from the cleavage reaction were collected, combined with trifluoroacetic acid washes of the resin, concentrated under reduced pressure, and treated with cold ether to precipitate the crude product.

Purification and Characterization. The crude peptide so obtained was purified by reversed-phase HPLC (Hewlett-Packard Series 1050) on a semipreparative Waters μ-Bondapack C18 (19 mm × 300 mm) column with detection at 220 nm. The crude product (50 mg) was dissolved in ∼4 mL of aqueous acetonitrile (20%) containing 0.025% TFA, applied to the column, and eluted with a water/acetonitrile linear gradient containing 0.025% TFA (0 to 70% acetonitrile over 2 h at a flow rate of 5 mL/min). The fractions were collected and analyzed at 220 nm by reversed-phase HPLC (Hewlett-Packard Series 1050) on an analytical Waters μ-Bondapack

Table 1: Bpa^x,Lys^7(biotinylamidocaproate)α-Factor Analogues, Yields of Biotinylation, and Results of Mass Spectral Analysis

	yield of biotinylated product (%)	purity (%) by HPLC	E_{280}[a]	MW (calculated)	ESI-MS[b]
Bpa^1,K^7(biotinylamidocaproate),Nle^{12},Y^{13}-α-factor (Bpa^1)	51.0[c]	>99	14 000	2070	2070.2
Bpa^3,K^7(biotinylamidocaproate),Nle^{12},Y^{13}-α-factor (Bpa^3)	89.9	>99	14 000	2070	2070.2
Bpa^5,K^7(biotinylamidocaproate),Nle^{12},Y^{13}-α-factor (Bpa^5)	90.2	>99	19 500	2128	2127.7
Bpa^8,K^7(biotinylamidocaproate),Nle^{12},Y^{13}-α-factor (Bpa^8)	86.2	>99	19 500	2159	2159.0
Bpa^{13},K^7(biotinylamidocaproate),Nle^{12}-α-factor (Bpa^{13})	84.1	>99	18 000	2093	2093.0

[a] The extinction coefficients were calculated with DNASTAR (Lasergene, Madison, WI) on the basis of the peptide sequence. [b] Mass spectral analysis of biotinylated analogues was performed by C. Soll (Hunter College, City University of New York). [c] This synthesis was not optimized.

C18 (3.9 mm × 300 mm) column. Fractions that were more than 99% homogeneous were pooled and subjected to lyophilization. The purity of the final peptide was assessed by analytical HPLC using two different solvent systems (10 to 55% acetonitrile gradient, 15 min, with 0.025% trifluoroacetic acid, and 50 to 80% methanol gradient, 30 min, with 0.025% trifluoroacetic acid) and ESI-MS (Hunter College, City University of New York, New York, NY).

Biotinylation of N-α-Fmoc-Protected α-Factor Analogues. Biotinylation of N-α-Fmoc-protected α-factor analogues was carried out using biotinylamidocaproate *N*-hydroxysuccinimide ester (Sigma). The N-α-Fmoc-protected α-factor analogue (10.0 mg, 5 μmol) was dissolved in 0.5 mL of cold (0 °C) DMF, and then the same volume (0.5 mL) of cold buffer ($Na_2B_4O_7$, pH 9.5, 50 mM) was added. The solution was stirred at 0 °C (ice bath) for 2 min, and 10.0 mg (20 μmol) of biotinylamidocaproate *N*-hydroxysuccinimide ester (Sigma) dissolved in 0.5 mL of cold DMF (0 °C) was added very slowly. The reaction was monitored by analytical reversed-phase HPLC using a linear gradient of 20 to 70% ACN in 30 min, and when the starting peptide disappeared (20−40 min) 0.5 mL of a 20% solution of piperidine in DMF was added and the reaction mixture was stirred at room temperature for 30 min until the Fmoc group was fully deprotected, as monitored by analytical HPLC. The reaction mixture was neutralized with 0.2 M HCl, and injected immediately onto a preparative HPLC column (conditions for preparative HPLC, 20 to 70% ACN over 150 min; column, Waters μ-Bondopack C18, 19 mm × 300 mm). The main fraction was collected and lyophilized. The purity of the biotinylated peptide was >99% as determined by analytical HPLC, and the molecular weight of peptide was confirmed by mass spectral analysis. The overall recovery of the purified biotinylated peptide was 85−90%.

Growth Arrest (Halo) Assay. Solid MLT medium [6.7 g/L yeast nitrogen base without amino acids (Difco), 10 g/L casamino acids (Difco), 20 g/L glucose, 0.058 g/L adenine sulfate, 0.026 g/L arginine, 0.058 g/L asparagine, 0.14 g/L aspartic acid, 0.14 g/L glutamic acid, 0.028 g/L histidine, 0.058 g/L isoleucine, 0.083 g/L leucine, 0.042 g/L lysine, 0.028 g/L methionine, 0.69 g/L phenylalanine, 0.52 g/L serine, 0.28 g/L threonine, 0.042 g/L tyrosine, 0.21 g/L valine, and 0.028 g/L uracil] (*35*) was overlaid with 4 mL of a *S. cerevisiae* DK102pNED cell suspension (2.5×10^5 cells/mL of Nobel agar). Filter disks (sterile blanks from Difco), 8 mm in diameter, were impregnated with 10 μL portions of peptide solutions at various concentrations and placed onto the overlay. The plates were incubated at 30 °C for 24−36 h and then observed for clear zones (halos) around the disks. The data were expressed as the diameter of the halo, which includes the diameter of the disk. A minimum value for growth arrest is 9 mm, which represents the disk diameter (8 mm) and a small zone of inhibition. All assays were carried out at least three times with no more than a 2 mm variation in halo size at a particular amount applied for each peptide. The reported values represent the mean of these tests.

Binding Competition Assay with [^{3}H]-α-Factor. This assay was performed using strain DK102pNED and tritiated α-factor prepared by reduction of [dehydroproline^8,Nle^{12}]-α-factor as described previously (*33*). In general, cells were grown at 30 °C overnight and harvested at a density of 1×10^7 cells/mL by centrifugation at 5000*g* and 4 °C. The pelleted cells were washed twice in ice-cold buffer [PPBi, 0.5 M potassium phosphate (pH 6.24) containing 10 mM TAME, 10 mM sodium azide, 10 mM potassium fluoride, and 1% BSA (fraction IV)] and resuspended at a density of 4×10^7 cells/mL. The binding assay was started by addition of [^{3}H]-α-factor (6 nM) and various concentrations of nonlabeled peptide (140 μL) to a 560 μL cell suspension. Analogue concentrations were adjusted using UV absorption at 280 nm and the corresponding extinction coefficients (Table 1). After incubation for 30 min, triplicate samples of 200 μL were filtered and washed over glass fiber filtermats using the Standard Cell Harvester (Skatron Instruments, Sterling, VA) and placed in scintillation vials for counting. Each experiment was carried out at least three times with similar results in each assay. The K_i values were calculated by using the equation of Cheng and Prusoff, where $K_i = IC_{50}/(1 + [\text{ligand}]/K_m)$ (*36*).

Cross-Linking of α-Factor Analogues to Ste2p. BJS21 and BJS21 pNED membranes (220 μg/mL of total protein) (*31*) were incubated with 975 μL of PPBi buffer (with 0.1% BSA) in siliconized microfuge tubes for 10 min at ambient temperature. Bpa-scanned biotinylated α-factor analogues (10 nM Bpa1, Bpa3, or Bpa13 and 20 nM Bpa5 or Bpa8) were added, and the reaction mixture was incubated for 30 min at room temperature with gentle mixing. The reaction mixture was aliquoted into three wells of a chilled 24-well plastic culture plate preblocked with PPBi (0.1% BSA). Division of the reaction mixtures into separate wells kept the depth of the samples minimal for efficient UV penetration of the sample. The samples were held at 4 °C and irradiated without the culture plate lid at 365 nm for 45 min in the case of Bpa1, Bpa3, or Bpa13 and for 90 min for Bpa5 or Bpa8 at a distance of 12 cm in a Stratlinker (Stratagene, La Jolla, CA). Membrane samples were recombined in siliconized microfuge tubes and washed twice by centrifugation (14000*g*) with PPBi (0.1% BSA). Membrane pellets were dissolved in 5 μL of sample buffer [0.25 M Tris-HCl (pH 8.8), 0.005%

bromophenol blue, 5% glycerol, 1.25% β-mercaptoethanol, and 2% SDS]. Samples were heated to 37 °C for 10 min and separated by SDS−PAGE (10% gel, 30 mA). In competition cross-linking experiments, 100× cold α-factor was added together with biotinylated peptide. For subsequent receptor digestion analysis, the band between 45 and 60 kDa covering the cross-linked Ste2p mass was excised and placed into dialysis tubing (molecular weight cutoff of 30 000) with buffer [0.2 M Tris-acetate (pH 7.4), 1.0% SDS, and 100 mM dithiothreitol]. Electroelution was performed by placing dialysis tubing that contains the gel in a horizontal electrophoresis chamber with running buffer [50 mM Tris-acetate (pH 7.4), 0.1% SDS, and 0.5 mM sodium thioglycolate]. Elution was carried out at 100 V for 3 h. The buffer in the dialysis tubing was transferred to a Millipore Ultrafree-15 centrifuge filter device (molecular weight cutoff of 30 000) and concentrated by centrifugation. The concentrated sample was washed three times with 50 mM Tris-HCl (pH 7.5). The cross-linked samples were resolved with SDS−PAGE, transferred to a PVDF membrane, and assayed for the detection of proteins that are covalently linked with biotinylated analogues with the NeutrAvidin−HRP conjugate (NA−HRP) (Pierce). All the gels used in these blots were analyzed by staining with coomassie blue to ensure efficient transfer of the protein to the membrane.

Digestion of Cross-Linked Ste2p. Cross-linked samples were digested with CNBr, trypsin, or BNPS-skatole. For CNBr digestion, samples were dissolved in 70% formic acid, and 200 mg/mL CNBr was added. For trypsin digestion, samples were dissolved in trypsin digestion buffer [100 mM Tris-HCl (pH 8.5)], and 6.25 μg of trypsin (sequencing grade modified trypsin, Roche) was added to 250 μg of total proteins; after incubation for 6 h, a second batch of trypsin (6.25 μg) is added to achieve complete digestion. Ste2p contains a lysine residue (K269) followed by a proline residue (P270) in extracellular loop 3, which makes it less likely to be digested by trypsin. Nevertheless,we found that this region is reproducibly susceptible to trypsin digestion under the conditions described above. For BNPS-skatole digestion, samples were dissolved in 50% acetic acid with addition of 10 mg/mL BNPS-skatole. To prevent anomalous cleavage of Ste2p at histidine and tyrosine residues, 100-fold molar excess of tyrosine was added to the reaction mixture during BNPS-skatole digestion (*37*). Deglycosylated samples for BNPS-skatole digestion were prepared by treatment with PNGase F (500 units/μL, BioLabs). Briefly, ∼10 μL of partially purified Ste2p-containing membrane proteins (1 μg/μL) was incubated with 5 μL of 10× glycoprotein denaturing buffer (5% SDS and 10% β-mercaptoethanol) at 100 °C for 10 min. After 10 min, 5 μL of 10× G7 buffer [0.5 M sodium phosphate (pH 7.5)] and 5 μL of 10% NP-40 were added. Finally, 5 μL of PNGase F and 20 μL of water were added (total volume, 50 μL), and the mixture was incubated at room temperature overnight. All digestion reactions took place under nitrogen and in complete darkness at 37 °C. After digestion, samples were dried by vacuum centrifugation, resuspended in 50 μL of 0.5 M Tris (pH 8.25), and re-dried. The digested samples were dissolved in loading buffer (Bio-Rad) and resolved on 12% NuPAGE Bis-tris gels with MES running buffer (Invitrogen).

RESULTS

Synthesis of α-Factor Analogues. N-α-Fmoc-protected α-factor analogues containing Bpa[1], Bpa[3], Bpa[5], Bpa[8], or Bpa[13] were prepared by automated solid-phase synthesis using standard coupling and deprotection protocols. During several of the syntheses, we noted partial Fmoc removal occurred using the "complete wash protocol" of the Applied Biosystems 433A synthesizer. This problem was eliminated by washing with only DCM. N-α-Fmoc-protected Bpa-containing α-factor analogues were purified by semipreparative HPLC (Waters μ-Bondopack C_{18}, 125 Å, 19 mm × 300 mm, gradient from 20 to 60% acetonitrile over 150 min). After lyophilization, they were used in the synthesis of the corresponding biotinyl-amidocaproate (BioACA) derivatives. Thus, all biotinylated analogues used in this study were biotinylated at the ϵ-amine of Lys[7], and a spacer was used to ensure that the biotin group was available to the avidin detection protein. The final products containing both Bpa and biotin were more than 99% pure as determined by analytical reversed-phase HPLC and had the expected molecular weight (Table 1).

Receptor Affinities of Bpa-Scanned Biotinylated α-Factor Analogues. To achieve efficient cross-linking of a ligand to its receptor, it is necessary to employ ligand analogues that bind tightly. Previous studies showed that Bpa replacements were tolerated well at positions 1 (Trp), 3 (Trp), 5 (Gln), 7 (Lys), 8 (Pro), 12 (Met), and 13 (Tyr) of α-factor pheromone, with K_d values indicating 4−45-fold poorer binding in comparison to that of α-factor (*30*). On the basis of these data and our current working model for pheromone binding to receptor (*38*), we chose photo-cross-linkable analogues with Bpa at positions 1, 3, 5, 8, and 13 to determine points of contact between the peptide and its receptor. This placed potential cross-link sites in side chains throughout the pheromone. The position 7 side chain was used for the biotin tag for detection purposes (*39*).

Binding affinities of the Bpa-scanned biotinylated α-factor analogues were determined by assessing their ability to compete with [^{3}H]-α-factor as described in Experimental Procedures. Analogues containing Bpa[1] and Bpa[5] exhibited an only 3−4-fold reduction in binding affinity compared to that of the native α-factor (Figure 1 and Table 2). The binding affinity for Bpa[13] was relatively poor (∼12-fold lower than that of the wild type). [Bpa[8]]-α-Factor showed very poor competition and did not compete fully at the highest tested concentration, making the binding affinity for this analogue only an estimate. [Bpa[3]]-α-Factor exhibited a comparatively intermediate binding affinity of ∼40 nM, although this is also only an estimate as full competition did not occur at the highest tested concentration.

Bioactivities of Bpa-Scanned Biotinylated α-Factor Analogues. For the cross-linking studies to relate to a biologically relevant receptor−ligand interaction, it is important to determine whether the ligand has biological activity. Therefore, we investigated the ability of the Bpa/biotinylated α-factor analogues of this study to cause growth arrest of *MAT**a*** cells. Semilogarithmic plots of halo diameter versus the amount of peptide applied to the disk were all linear and exhibited similar slopes (data not shown). All analogues used in this assay were stable to enzymatic cleavage under the conditions that were tested as strains used in this analysis

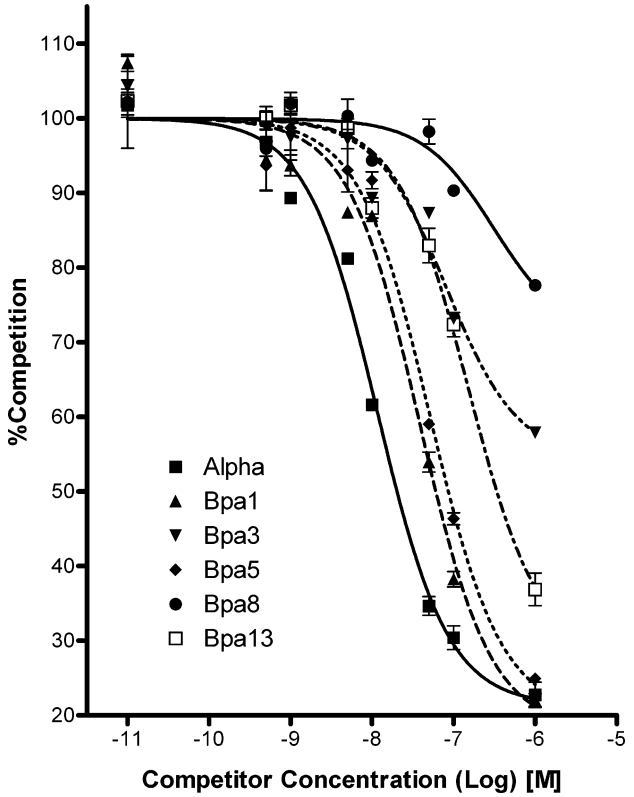

FIGURE 1: Competition binding assay of various α-factor analogues vs tritiated α-factor. Competitors were cold α-factor (■), Bpa1 (▲), Bpa3 (▼), Bpa5 (◆), Bpa8 (●), and Bpa13 (□).

Table 2: Summary of Receptor Affinities and Biological Activities for Bpa-Scanned Biotinylated α-Factor Analogues

	wild type	Bpa[1]	Bpa[3]	Bpa[5]	Bpa[8]	Bpa[13]
K_i (nM)	6	20	~40	25	~160	75
biological activity[a]	0.4	1.5	3.5	9.4	~50[b]	9
% affinity	100	30	15	24	~4	8
% activity	100	23	10	4	<1	5

[a] Amount of analogue (micrograms) needed to form a 15 mm halo of growth arrest. [b] Out of the linear range, the largest amount (20 μg) tested in this assay gave an only 13 mm halo.

lacked the Bar1p protease that cleaves α-factor. Therefore, the growth arrest data are indicative of the relative agonist activity of each peptide. The data show that the biotinylated peptides, where Bpa is at position 1, 3, 5, or 13, retained detectable agonistic activity, although the Bpa[3], Bpa[5], and Bpa[13] pheromones had a relatively poor ability to trigger signal transduction (Table 2). On the other hand, biotinylated [Bpa[8]]-α-factor did result in a small halo (~2 mm around the filter disk) at the highest concentration (20 μg/disk) used in this assay. None of the α-factor analogues induced growth arrest in a mutant lacking Ste2p (BJS21), confirming that the α-factor receptor was required for the biological activity of these peptides.

Cross-Linking of Bpa-Scanned Biotinylated α-Factor Analogues to Ste2p. The membranes derived from cells with a deletion in the α-factor receptor encoding gene *STE2* (BJS21) and membranes from these same cells transformed with a plasmid (pNED) encoding Ste2p (BJS21 pNED) were incubated with Bpa-scanned biotinylated α-factor analogues, and cross-linking was carried out using UV light (365 nm). BJS21 membranes were used as a control in this experiment to check the possible interference from the endogenous biotin

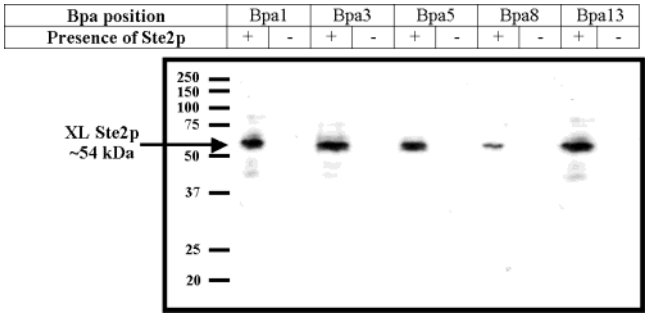

FIGURE 2: Western blot analysis of BJS21 pNED (expresses Ste2p) and BJS21 (ΔSte2p) photo-cross-linked membranes. Membranes photo-cross-linked with various Bpa-containing α-factor analogues were dissolved in Tricine sample buffer and resolved with a SDS-PAGE 10% gel. Proteins were transferred to a PVDF membrane and probed with NA−HRP to detect the biotin signal on the analogue.

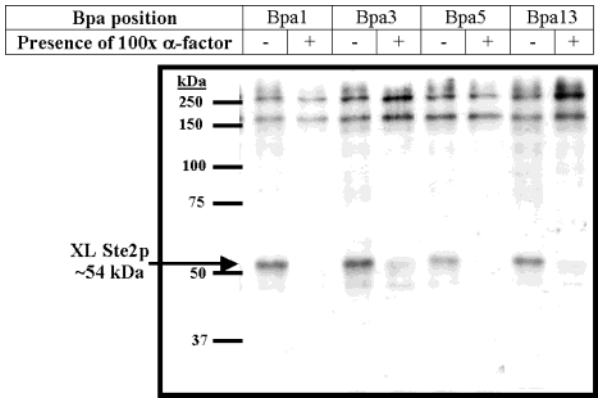

FIGURE 3: Western blot analysis of BJS21 pNED photo-cross-linked membranes in the presence or absence of excess wild-type α-factor. Membranes photo-cross-linked with various Bpa-containing α-factor analogues either in the presence or in the absence of 100× excess wild-type ligand and resolved with a SDS-PAGE 10% gel. Proteins were transferred to a PVDF membrane and probed with NA−HRP to detect the biotin signal on the analogue.

signal and/or nonspecific cross-linking products. Aliquots from each reaction mixture were removed following cross-linking and tested for incorporation of the biotinylated ligand into Ste2p by Western blot analysis probed with NA−HRP (Figure 2). The cross-linked product (54 kDa), which migrated to the expected size of Ste2p (52 kDa) with α-factor analogue (2 kDa), was detected in all lanes that contained cross-linked BJS21 pNED membranes, although the [Bpa[8]]-α-factor analogue exhibited a low degree of cross-linking consistent with its low biological activity and poor binding data. During the scanning of the film for preparation of the figure, a doublet seen for Ste2p on the original gels faded into the broader single band seen at ~54 kDa. No detectable signal was present on lanes loaded with BJS21 membranes (that lack Ste2p). In addition, no cross-linked products were visible with samples that were not UV-irradiated (data not shown).

In a follow-up experiment, the BJS21 pNED membranes were co-incubated with Bpa-scanned biotinylated α-factor analogues and a 100-fold molar excess of wild-type α-factor pheromone (Figure 3). Results indicated that in the presence of excess α-factor pheromone the level of cross-linking of the biotinylated analogues was greatly diminished, indicating that the cross-linking to Ste2p with the Bpa-scanned biotinylated α-factor analogues occurs at the α-factor binding

site. Cross-linking of [Bpa[8]]-α-factor was not blocked by addition of a 100-fold molar excess of α-factor (data not shown). We concluded that the small amount of cross-linking observed with the Bpa[8] analogue (Figure 2) may not reflect interaction with the α-factor binding site. This conclusion is supported by the relatively poor competition of this analogue for α-factor binding (Figure 1) and the poor biological activity of this analogue (Table 2). Therefore, further investigations with this probe were discontinued. Cross-linking of [Bpa[5]]-α-factor was blocked by excess α-factor; however, the amount of cross-linked product was very small in comparison to the amount of cross-linked product using Bpa[1], Bpa[3], and Bpa[13] analogues (Figure 3). Therefore, further experiments using this analogue were also not performed.

The cross-linking efficiency for the Bpa[1] analogue was determined as follows (data not shown). After [Bpa[1]]-α-factor had been cross-linked to FLAG-tagged Ste2p, membranes were solubilized and incubated with monomeric avidin beads. The flow-through washes (to elute un-cross-linked Ste2p) and acetonitrile/TFA washes (to disrupt noncovalent interactions between the cross-linked ligand−Ste2p complex and avidin and thereby elute Ste2p that was photo-cross-linked to biotinylated α-factor) were concentrated by vacuum centrifugation and resolved by SDS−PAGE. The proteins were then transferred to a PVDF membrane and probed with either NA−HRP or FLAG antibody. The NA−HRP blot indicated that cross-linked Ste2p (∼50 kDa band of Ste2p−Bpa−α-factor) was present only in the acetonitrile/TFA elution. A blot probed with FLAG antibody showed that a band at ∼50 kDa (Ste2p) was detected in the flow-through and acetonitrile elution, and comparison of the band intensities showed that ∼50% of the total Ste2p was cross-linked and retained by the monomeric avidin column. In an additional experiment, the cross-linking efficiency for Bpa[1], Bpa[3], and Bpa[13] analogues was estimated to be around 50% by comparison of the chemiluminescence signals from two different blots, one probed with NA−HRP (to detect cross-linked Ste2p by the reaction with the biotinylated analogue) and the other probed with a FLAG antibody detected by anti-mouse IgG HRP (to detect the total FLAG-tagged Ste2p). Since both experiments gave similar efficiencies for the Bpa[1] analogue, we conclude that the estimation of the efficiencies for the Bpa[3] and Bpa[13] analogues by this less direct comparison is also correct.

Fragmentation Analysis of Cross-Linked Ste2p. Membranes containing Ste2p (BJS21 pNED) cross-linked with various Bpa-scanned analogues described in this study were resolved by preparative SDS−PAGE. Cross-linked Ste2p was electroeluted from the gel and was treated with various cleavage agents to identify a fragment that covalently attached to the biotinylated ligand. Fragments of the cross-linked receptor were analyzed after trypsin, CNBr, and BNPS-skatole digestion to identify a putative Bpa[1], Bpa[3], and Bpa[13] cross-linked fragment(s). Trypsin digestion of the cross-linked receptor was carried out with sequencing grade trypsin at 37 °C for 16 h. To monitor trypsin digestion, we used a T7 epitope-tagged Ste2p (*40*) and detected an ∼4 kDa band (residues 270−303 and a T7 tag) by a T7 antibody instead of an ∼8 kDa band (residues 240−303 and a T7 tag), indicating that the Lys−Pro site in the third extracellular loop was susceptible to complete trypsin digestion under current digestion conditions (data not shown). A similar unexpected trypsin digestion at a Lys−Pro bond was observed by others (*41*). Chemical cleavage was performed by CNBr or BNPS-skatole under strongly acidic conditions. BNPS-skatole digestion was carried out on native and deglycosylated Ste2p prepared by treatment of Ste2p with PNGase F. These methods were previously used in our lab and applied by other groups in studies on Ste2p (*30*, *42*, *43*).

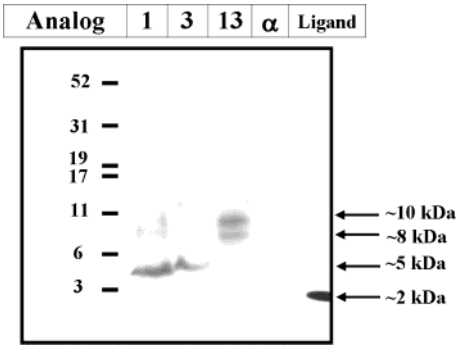

FIGURE 4: Western blot analysis of trypsin-digested BJS21 pNED photo-cross-linked membranes. Membranes photo-cross-linked with various Bpa-containing α-factor analogues were digested with trypsin and resolved with a Nu-PAGE 12% Bis-Tris gel. Proteins were transferred to a PVDF membrane and probed with NA−HRP to detect the biotin signal on the analogues. Membranes cross-linked with α-factor were used as a negative control, and ligand alone was used as a positive control.

Trypsin digestion resulted in fragments of ∼5 kDa for both Bpa[1] and Bpa[3] α-factor analogues, whereas ∼10 and ∼8 kDa bands for Bpa[13] α-factor were detected on the same blot (Figure 4). The theoretical digestion of Ste2p by trypsin shows multiple possible fragments that might correspond to 5 kDa after cross-linking with Bpa[1] or Bpa[3] (Figure 5A). CNBr digestion of the cross-linked receptor was carried out to narrow the putative cross-linked regions. Following CNBr digestion, a band of approximately 6 kDa was detected for both Bpa[1] and Bpa[3] (Figure 6). This result in combination with the trypsin digestion narrows the possible cross-linking to two regions, VIB (residues 190−218) or VIIIB (residues 251−294) (Figure 5B), where the latter is in agreement with our previous findings for Bpa[1] (*30*). CNBr digestion of Bpa[13]-cross-linked Ste2p resulted in an ∼3 kDa band (Figure 6). The overlapping region of the two digestions (trypsin and CNBr) corresponded to the region of Ste2p between residues F55 and R58 for Bpa[13] cross-linking. Further analysis of Bpa[13]-cross-linked Ste2p with BNPS-skatole was carried out. Digestion of the cross-linked native receptor resulted in two detectable bands around 12 and 10 kDa (Figure 7). Similar digestion with the deglycosylated receptor resulted in a single band around 10 kDa, indicating that Bpa[13] cross-linked to a glycosylated region of Ste2p represented by IC (residues 1−70 of Ste2p) (Figures 4C and 7). As a control to determine whether anomalous cleavage occurred with the BNPS-skatole reagent, we subjected the Bpa[1]-cross-linked receptor to fragmentation under similar conditions. In this case, only one band (∼27 kDa) was observed (Figure 7). Although one might predict that the BNPS-skatole reagent would cleave inside the peptide ligand thus releasing this ligand, we believe that the proximity of the cross-linked site (position 1) to Trp3 in the analogue might significantly slow this reaction.

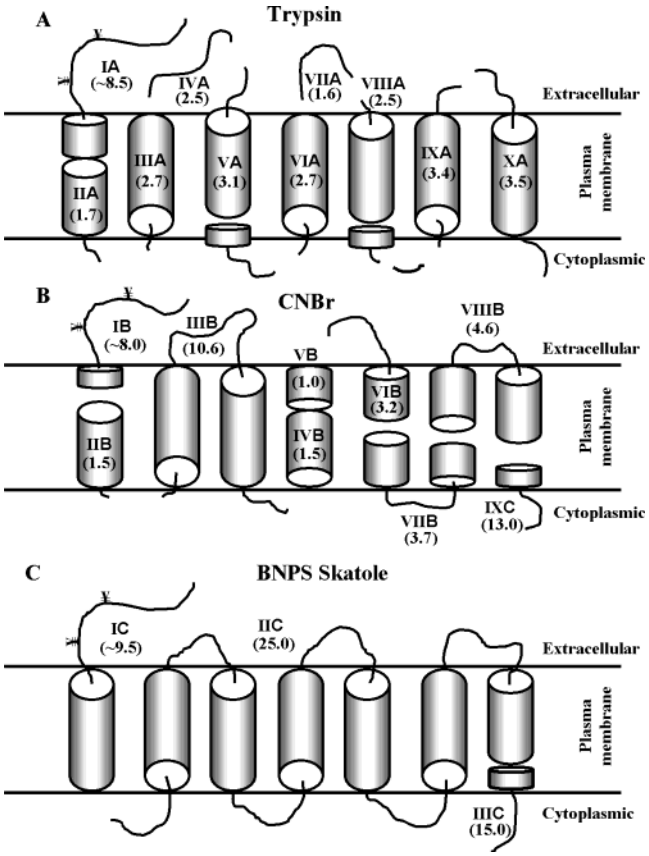

FIGURE 5: Schematic representation of receptor fragments after chemical and enzymatic cleavage of Ste2p. These figures represent the theoretical BNPS-skatole, trypsin, and CNBr cleavage sites for the Ste2p receptor. For the sake of simplicity, the cytoplasmic tail is not represented in these cartoons. (A) Peptides resulting from a complete trypsin digestion of Ste2p. (B) Receptor fragments generated after a complete CNBr cleavage of the receptor. (C) Cleavage of the receptor by BNPS-skatole results in four fragments, three of which represented IC (residues 1−70 of Ste2p), IIC (residues 71−295), and IIIC (residues 296−424). Molecular masses are represented on the figure in kilodaltons. N-Terminal fragments IA−IC contain two known N-linked glycosylation sites which adds ~2 kDa to these fragments; thus, the molecular masses for these fragments are approximations.

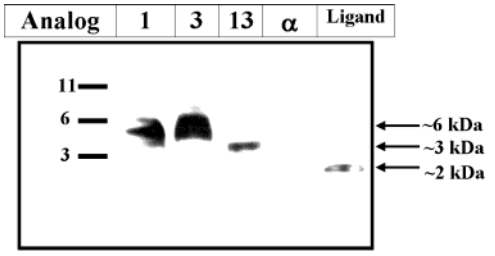

FIGURE 6: Western blot analysis of CNBr-digested BJS21 pNED photo-cross-linked membranes. Membranes photo-cross-linked with various Bpa-containing α-factor analogues were digested with CNBr and resolved with a Nu-PAGE 12% Bis-Tris gel. Proteins were transferred to a PVDF membrane and probed with NA−HRP to detect the biotin signal on the analogues. Membranes cross-linked with α-factor were used as a negative control, and ligand alone was used as a positive control.

DISCUSSION

This study details the synthesis and characterization of a new set of α-factor analogues containing Bpa as a photoactivatable cross-linker and biotin as a tag for detection. Photoaffinity labeling of receptor residues with Bpa has been

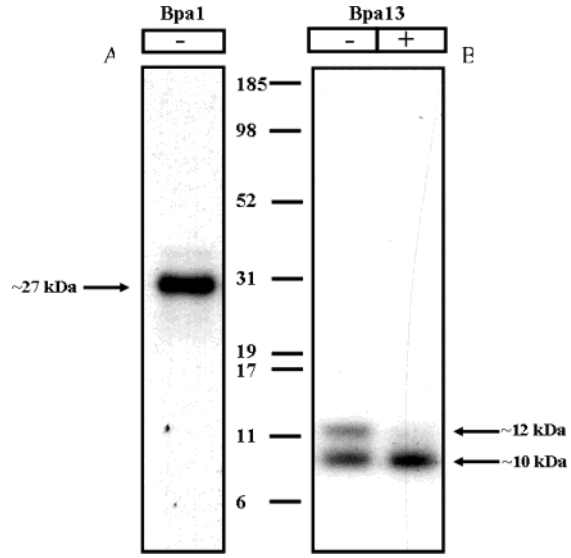

FIGURE 7: Bpa1- and Bpa13-cross-linked BJS21 pNED membranes [native (−) or deglycosylated (+)] were digested with BNPS-skatole (Pierce) for 16 h at 37 °C, then resolved with a 12% Bis-Tris gel (Invitrogen), and transferred to a PVDF membrane. Membranes were probed with NA−HRP conjugate to detect the biotin signal on the Bpa1 and Bpa13 analogues. (A) Band (~27 kDa) corresponding to a region of Ste2p between residues 71 and 295 (25 kDa) and the ligand (2 kDa). (B) The left lane is the BNPS-skatole digest of the native (−) membranes which generates two bands (~12 and ~10 kDa), and the right lane is the BNPS-skatole digest of the PNGase F-treated [deglycosylated (+)] membranes.

used as a powerful tool to obtain constraints to better understand the molecular basis of ligand binding and activation of receptors (*11*−*13*, *15*−*17*, *25*, *26*, *29*, *44*). Most of these studies used ^{125}I as a tag to track the cross-linking efficiency and detect the resulting cross-linked fragment after various chemical and enzymatic digestions for mapping the contact region. Our previous studies showed that iodination of Bpa-scanned α-factor analogues, except Bpa at position 1, resulted in either a loss of function due to multiple iodination or a drastic decrease in binding affinity, which made it impractical for cross-linking studies (*30*). Although biotin detection uses an indirect detection that includes transfer to membranes, probing with NA−HRP, and detection by a colorimetric enzymatic reaction compared to direct detection of radioiodine, the relatively unstable nature and high hydrophobicity of the ^{125}I-tagged ligand raised additional problems during comparison of consecutive experiments. Furthermore, in future investigations, biotinylated peptide fragments generated by chemical or enzymatic degradation can be isolated by affinity procedures and subjected to mass spectrometry. Therefore, in this study, we decided to use biotin instead of ^{125}I as a reporting tag with a series of Bpa-scanned α-factor analogues.

Early studies on the angiotensin II receptor (*45*) and recent work on chemotactic peptide analogues (*46*) and the integrin receptor (*47*) showed that biotin can be used as a reporting tag instead of radioactive isotopes. However, most of these studies were hampered by the low affinity of the ligand analogues due to incorporation of biotin as a reporter tag. Our results indicated that all of the Bpa/biotinylated analogues tested except Bpa^{8} retained binding affinities within approximately 1 order of magnitude of that of α-factor and were agonists (Table 2). Detection of the biotin tag was achieved with the NeutrAvidin−horseradish peroxidase

conjugate, which takes advantage of the strong interaction between the biotin and NeutrAvidin and a powerful reporting signal from the product of the peroxidase reaction thus avoiding the use of iodine at any point in the detection protocol.

Cross-linking experiments carried out with the membranes from a Ste2p knockout strain (BJS21) showed that under the conditions tested no nonspecific cross-linking or endogenous biotin signal in the region of Ste2p was detected (Figure 2). In addition, cross-linking of the biotinylated Bpa analogues to Ste2p was prevented by mixing a 100-fold molar excess of wild-type pheromone into the reaction mixture prior to UV irradiation (Figure 3). Thus, in principle, these α-factor analogues can be used to determine contacts between ligand side chains and receptor residues involved in binding interactions between α-factor and its GPCR Ste2p.

The [Bpa^5]-α-factor had good binding affinity but was a weak agonist (Table 2). Using an excess of ligand, we obtained reasonable cross-linking of this analogue (Figure 2). However, to obtain a detectable signal, an ∼2−4-fold higher concentration of Bpa^5 analogue was used compared to the other analogues, and the cross-linking time for this analogue was extended (longer UV exposure) to obtain a comparable cross-linking. Nevertheless, only limited amounts of cross-linked product were recovered from preparative gels, and digestion with both chemical and enzymatic reagents resulted in a loss of signal (data not shown). Considering our current working model, residue 5 of α-factor might be exposed to solvent or involved in interactions with the extracellular loops. Relative to the transmembrane (TM) domains, the loops are more mobile which might cause the environment around Bpa^5 to be more dynamic. Such mobility around Bpa^5 might influence cross-linking efficiency and thus hinder incorporation of Bpa^5-bound α-factor compared to the other analogues that seem to be interacting with the TMs. Supporting the lack of importance of the position 5 side chain in tight interactions with the binding site was our observation that the [L-Ala^5]-α-factor had the highest receptor affinity of any of the alanine-scanned α-factors (*48*). Thus, further analysis was not carried out with [Bpa^5]-α-factor, although we plan to revisit this issue if we can optimize cross-linking efficiencies in future studies. Due to a lack of detectable biological activity and poor competition between the [Bpa^8]-α-factor analogue and α-factor for receptor binding (Figure 1 and Table 2), fragmentation analysis for the receptor cross-linked with this analogue was also not carried out.

Trypsin digestion of the cross-linked receptor resulted in an ∼5 kDa band for both [Bpa^1]-α-factor and [Bpa^3]-α-factor analogues (Figure 4). The presence of multiple possible trypsin digestion fragments that could give a band around 5 kDa [IIIA−VIA and VIIIA−XA (Figure 5A) when cross-linked to the 2 kDa Bpa^1 or Bpa^3 analogues would give an ∼5 kDa fragment] made it very difficult to assign a cross-link region for Bpa^1 and Bpa^3 with only these results. On the other hand, when these results were combined with the CNBr digestion data, the region of the Ste2p interacting with [Bpa^1]-α-factor and [Bpa^3]-α-factor analogues was narrowed to two possibilities: a region covering part of EL2 and an extracellular portion of TM5 (Figure 5B, VIB) or part of TM6, EL3, and part of TM7 (Figure 5B, VIIIB). Previously, we determined that [Bpa^1]-α-factor cross-linked to a portion of Ste2p comprising TM6, EL3, and TM7 (*30*), in agreement with the second possibility mentioned above. If both N-terminal tryptophan residues of α-factor interact with the same portion of Ste2p, then [Bpa^3]-α-factor might interact as well with the TM6−EL3−TM7 region. However, on the basis of these experimental results, we cannot rule out the interaction of [Bpa^3]-α-factor with the EL2−TM5 region.

Trypsin digestion of the Bpa^{13}-cross-linked receptor resulted in bands of ∼8 and ∼10 kDa (Figure 4). After complete trypsin digestion of cross-linked Ste2p, there is only one theoretical Ste2p region that could give these bands with the cross-linked ligand: the glycosylated and unglycosylated N-terminus of the receptor (residues 1−58; Figure 5A, fragment IA) (*49*). Additional digestions with CNBr and BNPS-skatole were carried out to further probe the cross-linking. Detection of an ∼3 kDa band after CNBr digestion (Figure 6) in combination with two bands, ∼12 kDa (presumably the glycosylated N-terminal ∼10 kDa fragment with a ligand) and ∼10 kDa (the unglycosylated N-terminal fragment with a ligand) after BNPS-skatole digestion (Figure 7), strongly indicates that the N-terminus of the receptor was the region cross-linked with the [Bpa^{13}]-α-factor analogue. The higher intensity of the lower-molecular weight band observed in Figure 7 (middle lane) suggests one of two explanations. Glycosylation may interfere with either cross-linking efficiency or detection by NA−HRP. To further test whether the ∼12 kDa BNPS-skatole fragment was glycosylated, deglycosylation of the cross-linked receptor followed by BNPS-skatole digestion was carried out. Results showed that upon deglycosylation only a single band at ∼10 kDa was detected (Figure 7). Thus, we conclude that the [Bpa^{13}]-α-factor analogue interacts with the junction between the N-terminus of Ste2p and the start of TM1. The smallest overlapping region between the three different digestions (trypsin, CNBr, and BNPS-skatole) carried out with Ste2p cross-linked with the [Bpa^{13}]-α-factor analogue indicates that cross-linking occurs between residues F55 and R58. Although the Bpa^{13} analogue had a relatively greater loss in affinity and efficacy, almost complete competition with the wild-type ligand in a receptor binding assay, detection of biological activity by the halo assay, and prevention of cross-linking by an excess of α-factor indicated that this analogue interacted with the receptor in a manner similar to that of the wild-type ligand. Thus, information gathered from this ligand will be helpful in interpreting the possible contact(s) of position 13 of α-factor with its receptor Ste2p. Nevertheless, it is conceivable that the presence of the large diphenyl ketone group in the position 13 side chain does result in a reorientation of the peptide in the binding site. Only direct X-ray analysis on bound ligands can decide this issue. The identification of contacts between the position 1, 3, and 13 side chains of α-factor and specific regions of Ste2p leads us to refine our current working model (*30*) for the placement of the pheromone into its binding pocket on the receptor. Results presented herein indicate that the [Bpa^1]-α-factor analogue and the [Bpa^3]-α-factor analogue interact with the EL2−TM5 or TM6−EL3−TM7 region of Ste2p. In previous work from our laboratory using an iodinated [Bpa^1]-α-factor analogue, we showed a contact between position 1 of the ligand and the TM6−EL3−TM7 motif (30). Taken together, these and previous results suggest that the N-terminus of the pheromone interacts with a binding domain consisting of residues from the extracellular ends of TM5−TM7 and

portions of EL2 and EL3 close to these TMs. These conclusions are consistent with a previously proposed model (*50*) for the α-factor bound to Ste2p. Nevertheless, it is important to emphasize that the cross-linking results do not preclude other portions of Ste2p from participating in the binding domain for the N-terminus of α-factor.

This study also shows a direct interaction between the [Bpa^{13}]-α-factor analogue and a region of Ste2p at the extracellular end of TM1. Supporting this interaction are studies from our laboratory demonstrating that changes at both residue 58 in TM1 and position 13 of the ligand exhibit a similar phenotype. Preliminary studies by site-directed mutagenesis in TM1 show that mutation of the R58 residue (R58A, R58D, or R58E) results in a 25−100-fold decrease in binding affinity of the wild-type pheromone and an only 20−30% decrease in the biological activity determined by the halo assay (C. D. Son, unpublished results). Similarly, our previous work showed that position 13 analogues of α-factor, where Tyr was replaced with Ala or Ser, had very poor binding affinities but exhibited relatively good biological activity (*51*). Thus, our data from pheromone−receptor cross-linking studies, receptor mutagenesis analysis, and the structure−activity relationships of α-factor analogues would be consistent with an interaction between position 13 of the pheromone and TM1. We note that this conclusion conflicts with a previously reported hypothesis on a possible interaction between position 13 of α-factor and F204 (located at the extracellular end of TM5) of Ste2p (*50*). This hypothesis was mainly based on site-directed mutagenesis (F204C), resulting in a receptor defective in α-factor binding, and previous studies from our lab (*48*) showing defective binding of position 13 α-factor analogues. Considering our current working model and results presented in this study, an interaction between position 13 of α-factor and TM5 of Ste2p is unlikely.

Mutagenesis and α-factor analogue analysis concluding that residue Gln^{10} of α-factor interacts with Ste2p residues 47 and/or 48 (*38*) and that the N-terminus likely interacts with aromatic residues F262 and Y266 at the extracellular interface of TM6 (*30*, *50*), fluorescence spectroscopy studies indicating that the side chain of Lys^{7} of α-factor faces toward a pocket formed by extracellular loops (*52*), and cross-linking analysis suggesting that Trp^{1}, Trp^{3}, and Tyr^{13} of the pheromone interact with TM6−EL3−TM7, EL2−TM5 or TM6−EL3−TM7, and TM1 regions of Ste2p, respectively, have led us to refine our working model for fitting the tridecapeptide into the pheromone binding site (Figure 8). This model has a contact of Tyr^{13} of the pheromone with Ste2p residues between F55 and R58, an interaction between pheromone residue Gln^{10} with receptor residues S47 and/or T48, contacts of residues Trp^{1} and Trp^{3} of α-factor with F262 and Y266 of Ste2p, and a β-turn around the Pro-Gly sequence in the center of α-factor allowing the middle of the pheromone to interact with extracellular loops. Additional constraints of the bound structure should be forthcoming as we refine cross-linking studies with Bpa^{3} and Bpa^{5} analogues and sequencing analysis of the cross-linked fragments by mass spectrometry currently in progress in our laboratory.

Understanding how G protein-coupled receptors are activated by ligand binding is an important goal of workers in the GPCR field. A *de novo* computer model of Ste2p in the resting state (G. Nikiforovich, unpublished data) suggests

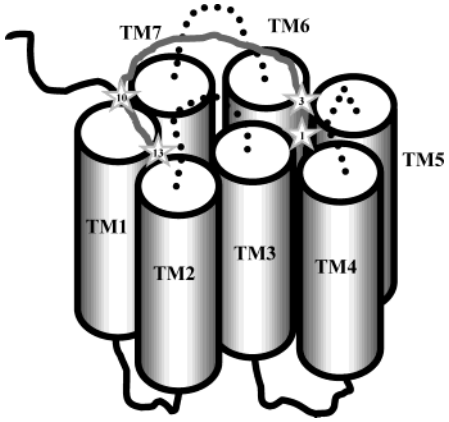

FIGURE 8: Working model for the fitting of the α-factor pheromone into the ligand binding site on its GPCR Ste2p. The α-factor and the loops are represented by the gray curve and dotted lines, respectively. Contact residues identified in this study and previous studies are denoted with stars with the residue number of the pheromone.

that R58 and Y98 are sufficiently close to be involved in a cation−π interaction. An interaction between the Tyr^{13} of the pheromone and R58 of Ste2p, as described in the binding model presented herein, would disturb this cation−π interaction leading to a conformational change that might facilitate a receptor shift to a more active state. Mutational studies on Y98 showed that replacing this residue with a histidine resulted in a receptor that was weakly constitutive and supersensitive to pheromone (*53*), which supports the idea that Y98 is important for stabilizing the inactive state of Ste2p, perhaps by interacting with R58. Additional studies on this GPCR system should lead to valuable insights into the mechanism of GPCR activation by a peptide ligand.

CONCLUSION

This study reports on the use of Bpa-scanned, biotinylated α-factor analogues for determining the direct interactions between the peptide ligand (pheromone) and a domain of the GPCR Ste2p. Use of biotin as a substitute for ^{125}I for tagging the photo-cross-linkable ligands to study ligand−receptor interactions was successfully achieved. Future studies employing high-resolution mass spectral charactization of fragments should allow for identification of residue-to-residue interactions between the analogues used in this study and their GPCR. Such information will aid the mapping of the ligand-binding site of the Ste2p receptor and has the potential to provide key insights into peptide ligand-mediated activation of GPCRs. As a paradigm for a medium-sized peptide hormone, this information may ultimately lead the discovery of how peptide ligands initiate signal transduction through these important signal transduction proteins.

ACKNOWLEDGMENT

We thank Frank Mason for technical assistance and Ayca Akal-Strader for the help with R58 mutant strains.

REFERENCES

1. Dohlman, H. G. (2002) G proteins and pheromone signaling, *Annu. Rev. Physiol. 64*, 129−152.
2. Dohlman, H. G., Thorner, J., Caron, M. G., and Lefkowitz, R. J. (1991) Model systems for the study of seven-transmembrane-segment receptors, *Annu. Rev. Biochem. 60*, 653−688.

3. Elion, E. A. (2000) Pheromone response, mating and cell biology, *Curr. Opin. Microbiol. 3*, 573−581.
4. Konopka, J. B., and Fields, S. (1992) The pheromone signal pathway in *Saccharomyces cerevisiae*, *Antonie Van Leeuwenhoek 62*, 95−108.
5. Sprague, G. F., Jr. (1991) Signal transduction in yeast mating: receptors, transcription factors, and the kinase connection, *Trends Genet. 7*, 393−398.
6. Fredriksson, R., Lagerstrom, M. C., Lundin, L. G., and Schioth, H. B. (2003) The G-protein-coupled receptors in the human genome form five main families. Phylogenetic analysis, paralogon groups, and fingerprints, *Mol. Pharmacol. 63*, 1256−1272.
7. Lefkowitz, R. J. (1996) G protein-coupled receptors and receptor kinases: from molecular biology to potential therapeutic applications, *Nat. Biotechnol. 14*, 283−286.
8. Balakin, K. V., Tkachenko, S. E., Lang, S. A., Okun, I., Ivashchenko, A. A., and Savchuk, N. P. (2002) Property-based design of GPCR-targeted library, *J. Chem. Inf. Comput. Sci. 42*, 1332−1342.
9. Klabunde, T., and Hessler, G. (2002) Drug design strategies for targeting G-protein-coupled receptors, *ChemBioChem 3*, 928−944.
10. Fong, T. M., and Strader, C. D. (1994) Functional mapping of the ligand binding sites of G-protein coupled receptors, *Med. Res. Rev. 14*, 387−399.
11. Hadac, E. M., Pinon, D. I., Ji, Z., Holicky, E. L., Henne, R. M., Lybrand, T. P., and Miller, L. J. (1998) Direct identification of a second distinct site of contact between cholecystokinin and its receptor, *J. Biol. Chem. 273*, 12988−12993.
12. Dorman, G., and Prestwich, G. D. (2000) Using photolabile ligands in drug discovery and development, *Trends Biotechnol. 18*, 64−77.
13. Dong, M., Wang, Y., Hadac, E. M., Pinon, D. I., Holicky, E., and Miller, L. J. (1999) Identification of an interaction between residue 6 of the natural peptide ligand and a distinct residue within the amino-terminal tail of the secretin receptor, *J. Biol. Chem. 274*, 19161−19167.
14. Behar, V., Bisello, A., Rosenblatt, M., and Chorev, M. (1999) Direct identification of two contact sites for parathyroid hormone (PTH) in the novel PTH-2 receptor using photoaffinity cross-linking, *Endocrinology 140*, 4251−4261.
15. Shoelson, S. E., Lee, J., Lynch, C. S., Backer, J. M., and Pilch, P. F. (1993) BpaB25 insulins. Photoactivatable analogues that quantitatively cross-link, radiolabel, and activate the insulin receptor, *J. Biol. Chem. 268*, 4085−4091.
16. Mouledous, L., Topham, C. M., Mazarguil, H., and Meunier, J. C. (2000) Direct identification of a peptide binding region in the opioid receptor-like 1 receptor by photoaffinity labeling with [Bpa-(10),Tyr(14)]nociceptin, *J. Biol. Chem. 275*, 29268−29274.
17. Boucard, A. A., Wilkes, B. C., Laporte, S. A., Escher, E., Guillemette, G., and Leduc, R. (2000) Photolabeling identifies position 172 of the human AT(1) receptor as a ligand contact point: receptor-bound angiotensin II adopts an extended structure, *Biochemistry 39*, 9662−9670.
18. Girault, S., Sagan, S., Bolbach, G., Lavielle, S., and Chassaing, G. (1996) The use of photolabelled peptides to localize the substance-P-binding site in the human neurokinin-1 tachykinin receptor, *Eur. J. Biochem. 240*, 215−222.
19. Li, Y. M., Marnerakis, M., Stimson, E. R., and Maggio, J. E. (1995) Mapping peptide-binding domains of the substance P (NK-1) receptor from P388D1 cells with photolabile agonists, *J. Biol. Chem. 270*, 1213−1220.
20. Kage, R., Leeman, S. E., Krause, J. E., Costello, C. E., and Boyd, N. D. (1996) Identification of methionine as the site of covalent attachment of a *p*-benzoyl-phenylalanine-containing analogue of substance P on the substance P (NK-1) receptor, *J. Biol. Chem. 271*, 25797−25800.
21. Ji, Z., Hadac, E. M., Henne, R. M., Patel, S. A., Lybrand, T. P., and Miller, L. J. (1997) Direct identification of a distinct site of interaction between the carboxyl-terminal residue of cholecystokinin and the type A cholecystokinin receptor using photoaffinity labeling, *J. Biol. Chem. 272*, 24393−24401.
22. Kojro, E., Eich, P., Gimpl, G., and Fahrenholz, F. (1993) Direct identification of an extracellular agonist binding site in the renal V2 vasopressin receptor, *Biochemistry 32*, 13537−13544.
23. Schievano, E., Mammi, S., Carretta, E., Fiori, N., Corich, M., Bisello, A., Rosenblatt, M., Chorev, M., and Peggion, E. (2003) Conformational and biological characterization of human parathyroid hormone hPTH(1−34) analogues containing β-amino acid residues in positions 17−19, *Biopolymers 70*, 534−547.
24. Gensure, R. C., Shimizu, N., Tsang, J., and Gardella, T. J. (2003) Identification of a Contact Site for Residue 19 of Parathyroid Hormone (PTH) and PTH-Related Protein Analogs in Transmembrane Domain Two of the Type 1 PTH Receptor, *Mol. Endocrinol. 17*, 2647−2658.
25. Zang, M., Dong, M., Pinon, D. I., Ding, X. Q., Hadac, E. M., Li, Z., Lybrand, T. P., and Miller, L. J. (2003) Spatial approximation between a photolabile residue in position 13 of secretin and the amino terminus of the secretin receptor, *Mol. Pharmacol. 63*, 993−1001.
26. Bes, B., and Meunier, J. C. (2003) Identification of a hexapeptide binding region in the nociceptin (ORL1) receptor by photo-affinity labelling with Ac-Arg-Bpa-Tyr-Arg-Trp-Arg-NH_2, *Biochem. Biophys. Res. Commun. 310*, 992−1001.
27. Perodin, J., Deraet, M., Auger-Messier, M., Boucard, A. A., Rihakova, L., Beaulieu, M. E., Lavigne, P., Parent, J. L., Guillemette, G., Leduc, R., and Escher, E. (2002) Residues 293 and 294 are ligand contact points of the human angiotensin type 1 receptor, *Biochemistry 41*, 14348−14356.
28. Rihakova, L., Deraet, M., Auger-Messier, M., Perodin, J., Boucard, A. A., Guillemette, G., Leduc, R., Lavigne, P., and Escher, E. (2002) Methionine proximity assay, a novel method for exploring peptide ligand−receptor interaction, *J. Recept. Signal Transduction Res. 22*, 297−313.
29. Bisello, A., Adams, A. E., Mierke, D. F., Pellegrini, M., Rosenblatt, M., Suva, L. J., and Chorev, M. (1998) Parathyroid hormone-receptor interactions identified directly by photocross-linking and molecular modeling studies, *J. Biol. Chem. 273*, 22498−22505.
30. Henry, L. K., Khare, S., Son, C., Babu, V. V., Naider, F., and Becker, J. M. (2002) Identification of a contact region between the tridecapeptide α-factor mating pheromone of *Saccharomyces cerevisiae* and its G protein-coupled receptor by photoaffinity labeling, *Biochemistry 41*, 6128−6139.
31. David, N. E., Gee, M., Andersen, B., Naider, F., Thorner, J., and Stevens, R. C. (1997) Expression and purification of the *Saccharomyces cerevisiae* α-factor receptor (Ste2p), a 7-transmembrane-segment G protein-coupled receptor, *J. Biol. Chem. 272*, 15553−15561.
32. Guldener, U., Heck, S., Fielder, T., Beinhauer, J., and Hegemann, J. H. (1996) A new efficient gene disruption cassette for repeated use in budding yeast, *Nucleic Acids Res. 24*, 2519−2524.
33. Raths, S. K., Naider, F., and Becker, J. M. (1988) Peptide analogues compete with the binding of α-factor to its receptor in *Saccharomyces cerevisiae*, *J. Biol. Chem. 263*, 17333−17341.
34. Aletras, A., Barlos, K., Gatos, D., Koutsogianni, S., and Mamos, P. (1995) Preparation of the very acid-sensitive Fmoc-Lys(Mtt)-OH. Application in the synthesis of side-chain to side-chain cyclic peptides and oligolysine cores suitable for the solid-phase assembly of MAPs and TASPs, *Int. J. Pept. Protein Res. 45*, 488−496.
35. Bitan, G., Scheibler, L., Greenberg, Z., Rosenblatt, M., and Chorev, M. (1999) Mapping the integrin alpha V β3-ligand interface by photoaffinity cross-linking, *Biochemistry 38*, 3414−3420.
36. Cheng, Y., and Prusoff, W. H. (1973) Relationship between the inhibition constant (K1) and the concentration of inhibitor which causes 50% inhibition (I50) of an enzymatic reaction, *Biochem. Pharmacol. 22*, 3099−3108.
37. Durrer, P., Galli, C., Hoenke, S., Corti, C., Gluck, R., Vorherr, T., and Brunner, J. (1996) H^+-induced membrane insertion of influenza virus hemagglutinin involves the HA2 amino-terminal fusion peptide but not the coiled coil region, *J. Biol. Chem. 271*, 13417−13421.
38. Lee, B. K., Khare, S., Naider, F., and Becker, J. M. (2001) Identification of residues of the *Saccharomyces cerevisiae* G protein-coupled receptor contributing to α-factor pheromone binding, *J. Biol. Chem. 276*, 37950−37961.
39. Ding, F. X., Lee, B. K., Hauser, M., Patri, R., Arshava, B., Becker, J. M., and Naider, F. (2002) Study of the binding environment of α-factor in its G protein-coupled receptor using fluorescence spectroscopy, *J. Pept. Res. 60*, 65−74.
40. Dube, P., DeCostanzo, A., and Konopka, J. B. (2000) Interaction between transmembrane domains five and six of the α-factor receptor, *J. Biol. Chem. 275*, 26492−26499.
41. Kieliszewski, M. J., Leykam, J. F., and Lamport, D. T. (1989) Trypsin cleaves lysylproline in a hydroxyproline-rich glycoprotein from *Zea mays*, *Pept. Res. 2*, 246−248.

42. Bukusoglu, G., and Jenness, D. D. (1996) Agonist-specific conformational changes in the yeast α-factor pheromone receptor, *Mol. Cell. Biol. 6*, 4818−4823.
43. Konopka, J. B., Jenness, D. D., and Hartwell, L. H. (1988) The C-terminus of the *S. cerevisiae* α-pheromone receptor mediates an adaptive response to pheromone, *Cell 54*, 609−620.
44. Tan, Y. V., Couvineau, A., Van Rampelbergh, J., and Laburthe, M. (2003) Photoaffinity labeling demonstrates physical contact between vasoactive intestinal peptide and the N-terminal ectodomain of the human VPAC1 receptor, *J. Biol. Chem. 278*, 36531−36536.
45. Bonnafous, J. C., Tence, M., Seyer, R., Marie, J., Aumelas, A., and Jard, S. (1988) New probes for angiotensin II receptors. Synthesis, radioiodination and biological properties of biotinylated and haptenated angiotensin derivatives, *Biochem. J. 251*, 873−880.
46. Shibue, M., Yoshiki, M., Miyazaki, M., Fujita, I., Osada, S., Yasuda, S., Nakamura, H., Hamasaki, Y., Kondo, M., Maeda, H., Kodama, H., and Shimizu, H. (2003) Synthesis of chemotactic peptide analogs with a photoaffinity cross-linker as new probes for analysis of receptor−ligand interaction, *Protein Pept. Lett. 10*, 147−153.
47. Bitan, G., Scheibler, L., Teng, H., Rosenblatt, M., and Chorev, M. (2000) Design and evaluation of benzophenone-containing conformationally constrained ligands as tools for photoaffinity scanning of the integrin αVβ3-ligand bimolecular interaction, *J. Pept. Res. 55*, 181−194.
48. Abel, M. G., Zhang, Y. L., Lu, H. F., Naider, F., and Becker, J. M. (1998) Structure−function analysis of the *Saccharomyces cerevisiae* tridecapeptide pheromone using alanine-scanned analogs, *J. Pept. Res. 52*, 95−106.
49. Mentesana, P. E., and Konopka, J. B. (2001) Mutational analysis of the role of N-glycosylation in α-factor receptor function, *Biochemistry 40*, 9685−9694.
50. Lin, J. C., Parrish, W., Eilers, M., Smith, S. O., and Konopka, J. B. (2003) Aromatic residues at the extracellular ends of transmembrane domains 5 and 6 promote ligand activation of the G protein-coupled α-factor receptor, *Biochemistry 42*, 293−301.
51. Liu, S., Henry, L. K., Lee, B. K., Wang, S. H., Arshava, B., Becker, J. M., and Naider, F. (2000) Position 13 analogs of the tridecapeptide mating pheromone from *Saccharomyces cerevisiae*: design of an iodinatable ligand for receptor binding, *J. Pept. Res. 56*, 24−34.
52. Ding, F. X., Lee, B. K., Hauser, M., Davenport, L., Becker, J. M., and Naider, F. (2001) Probing the binding domain of the *Saccharomyces cerevisiae* α-mating factor receptor with fluorescent ligands, *Biochemistry 40*, 1102−1108.
53. Parrish, W., Eilers, M., Ying, W., and Konopka, J. B. (2002) The cytoplasmic end of transmembrane domain 3 regulates the activity of the *Saccharomyces cerevisiae* G-protein-coupled α-factor receptor, *Genetics 160*, 429−443.

BI0496889